Published in final edited form as:
Traffic. 2014 June ; 15(6): 684–699. doi:10.1111/tra.12169.

A 14-3-3 Mode-1 Binding Motif Initiates Gap Junction Internalization during Acute Cardiac Ischemia

James W. Smyth[1], **Shan-Shan Zhang**[1], **Jose M. Sanchez**[2], **Samy Lamouille**[2], **Jacob M. Vogan**[2], **Geoffrey G. Hesketh**[3], **TingTing Hong**[1,4], **Gordon F. Tomaselli**[3], and **Robin M. Shaw**[1,4,*]

[1]Heart Institute and Department of Medicine, Cedars-Sinai Medical Center

[2]Department of Medicine, University of California San Francisco

[3]Division of Cardiology, Johns Hopkins Medical Center

[4]Department of Medicine, University of California Los Angeles

Abstract

Altered phosphorylation and trafficking of connexin 43 (Cx43) during acute ischemia contributes to arrhythmogenic gap junction remodeling, yet the critical sequence and accessory proteins necessary for Cx43 internalization remain unresolved. 14-3-3 proteins can regulate protein trafficking, and a 14-3-3 mode-1 binding motif is activated upon phosphorylation of Ser373 of the Cx43 C-terminus. We hypothesized that $Cx43^{Ser373}$ phosphorylation is important to pathologic gap junction remodeling. Immunofluorescence in human heart reveals enrichment of 14-3-3 proteins at intercalated discs, suggesting interaction with gap junctions. Knockdown of 14-3-3τ in cell lines increases gap junction plaque size at cell-cell borders. $Cx43^{S373A}$ mutation prevents Cx43/14-3-3 complexing and stabilizes Cx43 at the cell surface, indicating avoidance of degradation. Using Langendorff-perfused mouse hearts we detect phosphorylation of newly internalized Cx43 at Ser373 and Ser368 within 30 minutes of no-flow ischemia. Phosphorylation of Cx43 at Ser368 by PKC and Ser255 by MAPK has previously been implicated in Cx43 internalization. The $Cx43^{S373A}$ mutant is resistant to phosphorylation at both these residues and does not undergo ubiquitination, revealing Ser373 phosphorylation as an upstream gate-keeper of a post-translational modification cascade necessary for Cx43 internalization. $Cx43^{Ser373}$ phosphorylation is a potent target for therapeutic interventions to preserve gap junction coupling in the stressed myocardium.

Keywords

Connexin; Gap Junction; 14-3-3; Ischemia; Endocytosis

[*]To whom correspondence should be addressed: Robin M. Shaw M.D. Ph.D, Cedars-Sinai Heart Institute / UCLA, 8700 Beverly Blvd, Suite Davis 1016, Los Angeles, CA 90048, phone: (310) 967-3842, fax: (310) 423-7637, Robin.Shaw@cshs.org.

The authors have no conflicts of interest to declare.

Introduction

Proper heart pumping function depends upon the organized and rapid propagation of action potentials through the working myocardium to induce coordinated organ level contraction. Coordination in heart ventricles, which are the main pumping chambers, is achieved primarily through direct electrical coupling of individual cardiomyocytes via connexin 43 (Cx43) gap junctions (1, 2). Gap junctions comprise thousands of intercellular channels which permit the rapid passage of cytosolic factors such as ions and second messenger signaling molecules. Individual connexin proteins oligomerize into hexameric transmembrane channels termed connexons. Once inserted into the plasma membrane, connexons then couple with connexons on the surface of neighboring cells to form gap junctions (3). There are 21 human connexin proteins, of which Cx43 is the most broadly expressed, and is particularly enriched in ventricular cardiomyocytes (4). Localization of Cx43 gap junctions to the intercalated discs of cardiomyocytes is essential for organ level propagation of action potentials. During stress, such as acute ischemia, Cx43 undergoes pathological remodeling and gap junction coupling is rapidly down-regulated (5–8). Such altered Cx43 localization slows action potential propagation and contributes to an arrhythmogenic substrate (2, 9–11).

The gap junction life cycle can be separated into three stages: (i) anterograde transport of *de novo* connexons from the Golgi apparatus to the cell surface, (ii) assembly into and maintenance within the gap junction plaque, and (iii) retrograde transport encompassing internalization prior to degradation (12–14). Alterations in the balance between any of these three stages can rapidly affect intercellular coupling as Cx43 has a relatively short half-life of 1–5 hours (15–17). We have previously demonstrated that altered regulation of the cytoskeleton-based forward trafficking machinery contributes to loss of Cx43 gap junction coupling in diseased hearts (11, 18). The Cx43 protein itself is subject to a host of posttranslational modifications which can influence its trafficking, conductance, and degradation (19). Of these modifications, phosphorylation of the Cx43 C-terminus has emerged as a powerful but complex mode of cellular gap junction regulation (20).

Several signal transduction pathways converge on the Cx43 C-terminus. Positive regulators of gap junction coupling include; protein kinase A (PKA) which promotes trafficking and assembly of gap junctions (21, 22), and casein kinase 1 (CK1) which also supports forward trafficking of Cx43 (23, 24) and was recently demonstrated to protect against arrhythmogenic internalization of gap junctions during stress (25). In contrast, phosphorylation of Cx43 by mitogen-activated protein kinase (MAPK) signaling reduces open channel probability and can induce internalization, ubiquitination, and degradation of Cx43 (26–31). Protein kinase C (PKC) phosphorylates Cx43 at Ser368 which reduces gap junction conductance in addition to promotion of Cx43 endocytosis and degradation (28, 32–37). Interestingly, $pCx43^{Ser368}$ is associated with cardioprotective effects such as reduction of infarct size, presumably by limiting the spread of toxic factors (38–40). Phosphorylation events on the Cx43 C-terminus can act as checkpoints in the regulation of subsequent posttranslational modification. For example, Ser368 phosphorylation itself is prevented by prior phosphorylation of the PKA site Ser365 (41).

In close proximity to Ser368 is residue Ser373 whose phosphorylation activates a 14-3-3 mode-1 binding motif (42, 43). 14-3-3 proteins are accessory proteins whose binding often requires phosphorylation of the client protein within a specific domain, which is the case with Ser373 of the Cx43 mode-1 binding motif. 14-3-3 proteins have diverse cellular functions, including regulation of vesicular transport (44). In terms of protein transport, 14-3-3 binding is associated with masking of endoplasmic reticulum (ER) retention motifs, promoting client protein trafficking through the vesicular transport pathway (44–46). Indeed, phosphorylation of Ser373 and Cx43/14-3-3 complexing has been implicated in the regulation of Cx43 anterograde transport (47, 48) and increased gap junction assembly during stress (49). Given the colocalization of 14-3-3 proteins with Cx43 at gap junction plaques (43), and increased phosphorylation of Ser373 during stress (49), we hypothesized that 14-3-3 complexes with Cx43 in gap junction plaques, and provides critical negative regulation during acute ischemia.

Results

14-3-3 proteins limit Cx43 gap junction plaque size

We chose to investigate the subcellular localization of 14-3-3 proteins in human heart relative to Cx43 distribution. By immunofluorescence, we find 14-3-3 proteins (green) throughout the cytosol of human adult cardiomyocytes, but also detect enrichment of 14-3-3 proteins which co-localizes with Cx43 at the intercalated disc (red, Figure. 1A, arrow). To investigate the potential role for 14-3-3 proteins in gap junction regulation, we exposed neonatal mouse ventricular cardiomyocytes (NVCMs) to the 14-3-3 inhibitor R18 (50). After 16 h of incubation with R18, Cx43 gap junction plaques (green) were substantially larger in comparison to control cells, as detected by immunofluorescence (Figure 1B). Seven isoforms of 14-3-3 exist in mammalian cells, with the 14-3-3τ isoform having previously been found to complex with Cx43 (43, 47, 49). Using siRNA-mediated knockdown of 14-3-3τ in a stable HaCaT cell line overexpressing Cx43, Western blotting reveals that loss of this 14-3-3 isoform increases total cellular Cx43 levels in comparison to cells transfected with a non-targeting siRNA (Figure. 1C). Cx43 protein exhibits a high turnover rate and one cellular location the protein can accumulate in the absence of degradation is the plasma membrane. We used fixed-cell immunofluorescence 24 hours post transfection with siRNA duplexes to identify where this stabilized pool of Cx43 protein occurs within the cell. Data presented in Figure. 1D reveal larger Cx43 gap junction plaques (green, arrows) following knockdown of 14-3-3τ (quantification in Figure 1E). Cell membrane is identified using wheat germ agglutinin (WGA, red). Taken together with the co-localization of 14-3-3 proteins and Cx43 at intercalated disc structures (Figure. 1A), these data suggest 14-3-3 binding limits gap junction plaque size at the cell surface.

Inactivation of the Cx43 14-3-3 binding motif increases Cx43 surface levels and stabilizes the Cx43 protein

14-3-3 complexing with partners such as Cx43 is dependent on phosphorylation of its binding motif (45, 51). The C-terminus of Cx43 contains a mode-1 14-3-3 binding motif whose activity requires phosphorylation of Ser373 (42) (Figure. 2A). Using site-directed mutagenesis, we substituted $Cx43^{Ser373}$ with the unphosphorylated mimetic alanine (S373A

mutation) to study the effects of inactivating the 14-3-3 binding motif on the Cx43 protein. Loss of the phosphorylated 14-3-3 motif was confirmed by immunoprecipitation followed by Western blot using a phosphorylation-specific antibody against the 14-3-3 mode-1 site (Figure. 2B, middle panel). In addition to ablation of a detectable 14-3-3 mode-1 binding motif, we find, by co-immunoprecipitation, that the $Cx43^{S373A}$ mutant has reduced affinity for 14-3-3τ in comparison to wild-type Cx43 (Figure. 2C, quantification in Figure 2D).

Given the increase in gap junction plaque size following knockdown of 14-3-3τ (Figure. 1C), we were interested if the S373A mutation, which limits 14-3-3τ binding to Cx43, could also increase Cx43 surface levels. HaCaT cells were transfected with either wild-type Cx43 or the $Cx43^{S373A}$ mutant 24 h prior to surface protein biotinylation. As seen in Figure. 3A, we detected a 41 % increase in surface levels of $Cx43^{S373A}$ compared to the wild type protein. Moreover, ^{35}S pulse chase experiments found the half-life of $Cx43^{S373A}$ to increase from 2.46 h to 3.48 h (Figure. 3B). The finding of increased Cx43 gap junction size upon loss of the 14-3-3τ isoform (Figure. 1C), and concomitant increase of both Cx43 surface levels (Figure. 3A) and half-life (Figure. 3B) upon mutation of the Cx43 14-3-3 binding motif, suggest that loss of 14-3-3/Cx43 interaction increases Cx43 stability.

Acute cardiac ischemia results in internalization of Cx43 phosphorylated at residues Ser368 and Ser373

Having found that Cx43/14-3-3 interaction regulates gap junction surface levels and Cx43 membrane stability, we were interested in the status of Ser373 phosphorylation during acute cardiac ischemia, when intercellular Cx43 gap junction coupling is actively undergoing not just altered forward trafficking (11) but remodeling from the intercalated disc by the cardiomyocyte (6). We exposed Langendorff-perfused mouse hearts to 30 minutes global ischemia or normal perfusion and harvested tissue for analysis by biochemistry and microscopy. Confocal immunofluorescence imaging of snap-frozen sections reveals lower levels of Cx43 (green) in colocalization with N-cadherin (red) at intercalated discs (Figure. 4A). SDS-PAGE of Cx43 typically exhibits four discrete bands termed p0, p1, p2, and p3 which are understood to represent various phosphorylation states (52). Following 30 minutes acute ischemia we find an increase in p0, p1, and p2 together with a loss of detectable p3 isoform (Figure. 4B). Despite this shift towards the faster migrating bands, we find that phosphorylation at Ser368 of Cx43 is significantly higher in ischemic hearts (Figure. 4C), and that this phosphorylation occurs in concert with phosphorylation of the Cx43 14-3-3 mode-1 binding motif at Ser373 (Figure. 4D). Having found that Ser373 phosphorylation reduces stability of surface membrane Cx43 (Figures 1–3) we examined whether ischemia induced phosphorylatation of membrane Cx43 may accelerate internalization.

Previous reports have localized $pCx43^{Ser368}$ to the intercalated disc following acute ischemia (53), and Cx43-Ser368 phosphorylation is involved in gap junction remodeling (38–40). Consistent with these reports, we find increased $pCx43^{Ser368}$ at intercalated discs as determined by immunofluorescence of frozen sections (Figure. 5A). High resolution confocal imaging uncovers an additional population of large $pCx43^{Ser368}$ (green) accumulatiions in close proximity to, but not within, the N-cadherin (red) enriched intercalated disc structures (arrows, Figure. 5B).

In order to investigate the origin of these non-junctional pCx43^{Ser368} structures and to complement imaging-based studies, we undertook biochemical tissue fractionation to localize Cx43 populations based upon triton-x100 solubility. Higher levels of pCx43^{Ser368} were detectable in the soluble (non-junctional) fraction after acute ischemia (Figure. 5C, quantification relative to total Cx43 in Figure. 5D). Additionally, more soluble Cx43 was phosphorylated in response to acute ischemia at Ser373 (mode-1, Figure. 5C and Figure. 5D). The acuity of the ischemic intervention (30 minutes) further indicates that the phosphorylation occurs on existing Cx43 that is internalized from the intercalated disc rather than on *de novo* generated Cx43. Taken together, these findings identify phosphorylation of Cx43 at the 14-3-3 mode-1 binding site Ser373, as well as Ser368, as occurring during acute cardiac ischemia and being associated with Cx43 internalization.

Cx43^{S373A} is resistant to PMA-induced phosphorylation, ubiquitination, and internalization

The Langendorff-perfused mouse heart studies in Figure. 4 and Figure. 5 reveal that internalized Cx43 is phosphorylated at Ser373 and Ser368 after 30 min acute ischemia. To test the relationship between these two sites and their role in Cx43 internalization, we used the phorbol ester PMA which is known to reduce gap junction coupling and induce ubiquitination and degradation of Cx43 in cultured cells. PMA activates protein kinase C (PKC) which, in turn, phosphorylates Cx43 at Ser368, leading to internalization (33). We exposed HaCaT cells transiently transfected with cDNA encoding wild-type Cx43 to PMA for 90 minutes. As expected, following stimulation we found surface levels of Cx43 were lower in PMA-stimulated cells (Figure. 6A). The decrease in surface levels were blocked using the endocytosis inhibitor Dynasore (54), confirming that PMA increases Cx43 internalization. The effects of PMA on Ser368 phosphorylation provides the opportunity to test whether Ser373 phosphorylation is upstream of Ser368. We repeated the experiment in Figure. 6A using the S373A mutant. Results, seen in Figure. 6B, are that S373A prevents PMA induced reductions in surface Cx43.

To study the effects of dynamic phosphorylation, we serum-starved HaCaT cells expressing wild-type Cx43 or Cx43^{S373A} and then stimulated them with PMA. The cells were harvested for biochemical analysis at multiple time points within a 2 hour period. Western blotting reveals that Ser368 is rapidly and robustly phosphorylated upon stimulation by PMA (left side of Figure. 6C red arrow, quantification in red line of graph). Interestingly, the Cx43^{S373A} mutant prevents Ser368 phosphorylation (right side of Figure. 6C red arrow, quantification in green line of graph). These findings confirm that Cx43 Ser368 phosphorylation is downstream of Cx43 Ser373 phosphorylation.

It is worth noting that, through a combination of stimulating Ser368 phosphorylation and activating of MAPK pathways, PMA also results in phosphorylation of Cx43 at Ser255 (28). Just as with Ser368 phosphorylation in Figure. 6C, we found the Cx43^{S373A} mutant resistant to phosphorylation at Ser255 when the cells were exposed to PMA (Figure. 7A). MAPK phosphorylation of Cx43 occurs upstream of ubiquitination and internalization (55). Immunoprecipitation of Cx43 to determine the ubiquitination status of the protein, reveals that the Cx43^{S373A} mutant is resistant to ubiquitination (Figure. 7B), in addition to upstream phosphorylation events at Ser373, Ser368 and Ser255. The finding that phosphorylation of

Ser373 is necessary for phosphorylation at Ser368/255, followed by ubiquitination of Cx43, indicates that Ser373 phosphorylation is a gatekeeper event for these highly important regulatory posttranslational events in intercellular gap junction coupling (Figure. 7C).

Discussion

Altered phosphorylation of Cx43 is a hallmark of the pathological remodeling of gap junctions during disease (6, 12, 20). Rather than individual phosphorylation events being independent of each other, it is likely that internalization results from a sophisticated cascade of posttranslational modifications. Here, we investigated the role of a phosphorylation-dependent 14-3-3 binding motif within the C-terminus of Cx43. 14-3-3 proteins are known to regulate protein transport, and have been implicated in facilitating *de novo* Cx43 transport from ER to Golgi apparatus (47, 48). In this study, we uncover an additional role for 14-3-3 binding at the Cx43 gap junction, where phosphorylation of Ser373 and 14-3-3 binding provides the gateway to a subsequent signaling cascade of downstream phosphorylation events leading to gap junction ubiquitination, internalization, and degradation during acute cardiac ischemia (Figure. 7C).

Investigating the effects of ablation of the Cx43 14-3-3 binding motif, through mutation of Ser373 to alanine, we find that Cx43 has higher surface expression and greater stability in the cell, consistent with 14-3-3 inhibition and knockdown data. Ser373 of Cx43 resides within a triad of double serines (Ser364/365, Ser368/369, Ser372/373) which are subject to dynamic phosphorylation events regulating gap junction formation (22, 24) and degradation (28, 33, 55, 56). Phosphorylation of Cx43-Ser365 is known to act as a gatekeeper, inhibiting phosphorylation of Ser368 by PKC (41). $pCx43^{Ser368}$ can lead to degradation of Cx43 (33, 36, 37) as well as reducing channel conductance (35). We uncover a sequential phosphorylation cascade initiating at Ser373 and continuing to PKC-mediated phosphorylation of Ser368, which is upstream of phosphorylation at Ser255. This is consistent with previous findings that Ser255 phosphorylation depends upon prior activation of PKC (28) and their promotion of gap junction degradation (55).

The Cx43 phosphorylation events described here negatively regulate Cx43 levels at the cell surface and therefore cell-cell coupling. In contrast, phosphorylation of Cx43 at Ser364 by PKA can promote gap junction assembly (22) and phosphorylation at Ser325/Ser328/Ser330 by CK1 also exerts positive effects on gap junction coupling (23). In a recent study, phosphomimetic mutation of Ser325/328/330 in a knock-in transgenic mouse model was found to limit pathological remodeling of Cx43 during pressure overload hypertrophy and protect against induced arrhythmia (25). Phosphorylation of Ser325/328/330 may occur as an important checkpoint in the cascade of events outlined in Figure. 7C which lead to gap junction internalization.

While posttranslational modification of the Cx43 C-terminus is clearly a potent mechanism for the cell to regulate gap junction coupling, transgenic mouse studies with Cx43 truncation mutants ($Cx43^{K258STOP}$) have revealed that the C-terminus is not necessary for Cx43 targeting to gap junctions, although alterations in gap junction size and localization were observed (57). Despite the presence of gap junctions, $Cx43^{K258STOP}$ mice were found more

susceptible to arrhythmia, and experienced increased infarct size following coronary occlusion (58). Such findings highlight the importance of the Cx43 C-terminus in the dynamic fine-tuning of gap junction coupling, whereby loss of the C-terminus potentially limits the cells capability to rapidly regulate gap junctions during stress. A more recent study ablating just the PDZ domain of Cx43, which is known to interact with ZO-1 for gap junction organization ($Cx43^{D378STOP}$), found that gap junctions were unaltered, but localization of $Na_V1.5$ was disrupted and mice were more susceptible to arrhythmias (59). Taken together, these studies raise the exciting possibility of a non-canonical scaffolding function for the Cx43 C-terminus in regulating cardiac intercalated disc function, which may relate to our recent finding of several N-terminally truncated Cx43 isoforms that are generated endogenously by internal translation of the Cx43 mRNA transcript (60).

We are finding Cx43 to be a powerful probe that, through the study of its lifecycle, is highlighting key regulatory mechanisms in protein regulation. Beginning at the ribosome with alternate translation (60), followed by hemichannel assembly in the ER/Golgi, cytoskeletal-based transport to the cell surface (11, 17, 18), non-canonical functions in the perinexus (61–63), accrual into gap junction plaques (49), internalization, degradation (33, 55, 64, 65), and recycling(66), it is very likely that 14-3-3 complexing may regulate phosphorylation, ubiquitination, and internalization of other proteins as well.

Phosphorylation of the Cx43 C-terminus can also alter Cx43 gap junction channel conductance (20). In this study, we report phosphorylation of Cx43 at Ser368 as an event which promotes internalization of gap junctions from the cell surface in human epithelial cells and in ischemic mouse heart. However, the $pCx43^{Ser368}$ has also been found to be cardioprotective, and can limit infarct size and arrhythmia (38–40). It is believed that these protective effects are mediated through reduced gap junction conductance, which limits the spread of toxic factors during stress (38). Protein phosphorylation is a highly dynamic process, can occur within seconds of kinase activation, and just as quickly be reversed through actions of protein phosphatases. It is important to consider that many studies on cardioprotection via $pCx43^{Ser368}$ are undertaken several days or longer post insult, when overall Cx43 phosphorylation status could be quite different compared to the acute scenario in this report. In this study, we have identified distinct populations of $pCx43^{Ser368}$ both within intercalated disc structures as previously reported and in cytosolic pools which we believe are internalized (Figure. 5). It is possible that those channels remaining in the intercalated disc may harbor alternative phosphorylated/dephosphorylated residues preventing their internalization, and therefore effecting cardioprotective effects of $pCx43^{Ser368}$ such as reduced conductance.

Cx43 has many binding partners within the cell, and the majority of these protein-protein interactions occur via the Cx43 C-terminus (67). In close proximity to the Cx43 14-3-3 binding motif studied here, is a PDZ domain encompassing the distal end of the C-terminus. It is through this PDZ domain that Cx43 interacts with another scaffolding protein, ZO-1 (68), and this interaction has been demonstrated to regulate Cx43 gap junction plaque size and assembly (69, 70). Disruption of Cx43/ZO-1 complexing has been reported to increase gap junction plaque size in cultured cells (71, 72). Phosphorylation of $Cx43^{Ser373}$ can disrupt interaction with ZO-1 (73), and indeed it would be sterically unlikely for both 14-3-3

and ZO-1 to bind the same Cx43 protomer simultaneously. Consistent with these reports, a recent study by Dunn and Lampe found that phosphorylation of Cx43-Ser373 by AKT resulted in larger gap junctions and a loss of Cx43/ZO-1 interaction (49). However, increased Cx43/ZO-1 interaction has also been associated with gap junction remodeling, highlighting the complex nature of these dynamic posttranslational and protein complexing events, as they occur at various stages in the Cx43 lifecycle (74-76).

This report reveals 14-3-3 proteins as regulators of membrane protein endocytosis. 14-3-3 interaction therefore likely relates to Cx43 ubiquitination and binding of other known downstream effectors of Cx43 endocytosis such as AP-2, Esp15, Dab2, and dynamin2 (12, 14). With the identification of a series of intramolecular checkpoints regulating sequential phosphorylation events, it may be best to consider entire distinct phosphorylation 'patterns' of Cx43 having specific effects. 14-3-3 proteins are also associated with positive regulation of Cx43 trafficking (48), implying multiple roles for the Cx43 mode-1 binding motif as the protein makes its way from the ER, to the cell surface, and back again. Also, the recent discovery of the dynamic perinexus region at the edge of the gap junction plaque provides support for multiple pools of Cx43 with distinct patterns of phosphorylated residues regulating scaffolding as well as entry and exit from the gap junction proper (62, 70). As the evidence in the work presented here suggests, Ser373 phosphorylation and 14-3-3 binding initiates this pathway, and may represent a potent target for therapies aimed at restoring normal gap junction coupling in heart disease.

Materials and Methods

Mice

C57BL/6 mice were maintained under sterile barrier conditions. All procedures were reviewed and approved by the University of California IACUC.

Human Tissue

With UCSF Committee for Human Research approval, the California Transplant Donor Network (CTDN) provided unused donor hearts and obtained informed consent for their use from the next of kin. Samples from left ventricle base were embedded in OCT medium and submerged in liquid N_2-chilled isopentane to snap-freeze before storage at −80°C.

Molecular Biology

Stealth siRNA duplexes targeting human *GJA1* (Cx43; HSS178257) and *YWHAQ* (14-3-3τ; HSS116960, HSS174015) were obtained from Life Technologies. Human *GJA1* for Cx43 expression was cloned using Gateway technology (Life Technologies) as previously described (9,18). Site-directed mutagenesis was performed using the QuickChange Lightning mutagenesis kit (Agilent Technologies). $Cx43^{S373A}$ mutation used the following sense: AGCAGTCGTGCCAGCGCCAGACCTCGGCCTGAT and antisense: ATCAGGCCGAGGTCTGGCGCTGGCACGACTGCT primers. Cx43 resistant to HSS178257 siRNA used the following sense: GTTGAGTCAGCCTGGGGCGACGAACAATCCGCA TTCCGCTGTAACACTCAGCAA and antisense:

TTGCTGAGTGTTACAGCGGAATGCGGATTGTTCG TCGCCCCAGGCTGACTCAAC primers.

Cell Culture

HaCaT cells were maintained in DMEM supplemented with 10% FBS, non-essential amino acids, sodium pyruvate (Life Technologies) and Mycozap (Lonza). Stable pLenti6.3-hCx43 expressing HaCaT cells were described previously (11). For knockdown studies, cells were reverse transfected with 10 nM siRNA using RNAiMAX (Life Technologies). Transfection of Cx43 cDNA was performed using Lipofectamine 2000 (Life Technologies). For stimulation assays, cells were serum-starved 24 hours post transfection for 4 hours prior to addition of PMA (100 nM).

P1 neonatal mouse ventricular cardiomyocytes (NMVMs) were isolated and maintained in culture as previously described (11, 18, 60). For 14-3-3 inhibition, cells were incubated for 16 h in the presence of R18 (25 μM, Sigma-Aldrich) or DMSO as vehicle control. Cells were fixed at room temperature for 30 min in 4% paraformaldehyde and immunofluorescence detection of Cx43 and N-cadherin performed as described below.

DSP-cross-linked co-immunoprecipitation

Transfected cells were incubated with DSP (Pierce) for 30 minutes at room temperature in PBS according to manufacturer's instructions. The reaction was quenched with 100 mM glycine in PBS and cells lysed in RIPA buffer as described above. Immunoprecipitation of lysates was undertaken using 2 μg mouse anti-14-3-3τ (Abcam) or mouse anti-GST (Santa-Cruz Biotechnology) as an isotype control. Protein complexes were precipitated using Dynabeads Protein G (Life Technologies) and washed four times in RIPA buffer. Elution was undertaken using 10 μl 2X NuPAGE sample buffer supplemented with 100 mM DTT and Western Blot performed.

^{35}S pulse chase

Transfected HaCaT cells in 100 mm dishes were starved in methionine- and cysteine-free medium containing 0.2% fetal bovine serum for 3 hours. The cells were then labeled with 0.15 mCi/ml [^{35}S]EXPRESS protein labeling mix (PerkinElmer) for 1 hour. Cells were washed three times with, and subsequently incubated in, fully supplemented DMEM. Dishes were sampled at 0, 3, 6, 9 and 12 hours post ^{35}S pulse. Upon sampling, cells were washed twice in ice-cold PBS and scraped into 500 μl RIPA. Lysates were clarified by centrifugation at 15,000 x *g* and precleared with 20 μl Protein G Sepharose 4B (Life Technologies). Immunoprecipitation was performed using 2 μg rabbit anti-Cx43 (Sigma-Aldrich) or rabbit anti-GST (Santa-Cruz Biotechnology) as an isotype control. Antibody/protein complexes were purified with 20 μl Protein G Sepharose 4B, and washed four times for 10 min in 1 ml RIPA. Immunoprecipitations were eluted into 10 μl 2X NuPAGE sample buffer supplemented with 100 mM DTT and subjected to SDS-PAGE. Labeled Cx43 was visualized using a phosphorimager, densitometry performed on resulting images using ImageJ software (NIH), and protein half-life calculated using non-linear regression analysis in Prism 5 software (Graphpad).

Surface Biotinylation

Surface proteins were biotinylated following 2 washes with ice-cold PBS by incubating cells for 5 minutes at 4°C with EZ-link Sulfo-NHS-SS-Biotin (Pierce Biotechnology) at a concentration of 0.5 mg/ml in PBS. Cells were washed in ice-cold PBS and incubated twice for 5 minutes in PBS containing 100 mM glycine to quench the reaction. After a further 2 washes in ice-cold PBS, cells were lysed in 200-μl RIPA buffer (50 mM Tris pH 7.4, 150 mM NaCl, 1 mM EDTA, 1% Triton X-100, 1% sodium deoxycholate, 2 mM NaF, 200 μM Na_3VO_4) supplemented with HALT Protease and Phosphatase Inhibitor Cocktail (Pierce Biotechnology). Lysates were sonicated using a Microson ultrasonic cell disruptor (Misonex) before centrifugation at 10,000 x *g* for 20 minutes at 4°C. Protein concentration was determined using the BioRad D_C Protein Assay and normalized. 1 mg of protein per condition was nutated with 50 μl of Ultralink Immobilized NeutrAvidin slurry (Pierce Biotechnology) overnight at 4°C. Beads were pelleted at 300 x *g* for 5 minutes and washed three times in 1 ml RIPA buffer. Bound proteins were eluted in 20 μl 2X NuPAGE sample buffer (Life Technologies) supplemented with 100 mM DTT (Sigma-Aldrich). Samples were heated for 10 minutes at 70°C prior to subjection to SDS-PAGE electrophoresis and Western blotting.

Langendorff-perfused mouse heart acute ischemia studies

8-week old Male C57BL/6 mice were anesthetized with isoflurane and injected with heparin (50 IU i.p.). After cervical dislocation, hearts were removed quickly by a midsternal incision and placed into ice-cold modified Krebs-Henseleit (K-H) solution. Under a dissecting microscope, the aortic opening was immediately cannulated and tied on a 23-gauge stainless steel blunt needle. The heart was attached to a Langendorff apparatus (ADInstruments) and perfused through the aorta at a constant rate of 4 ml/min with a modified pH 7.4 K-H buffer of the following composition (in mM): NaCl 118, KCl 4.7, $CaCl_2{\cdot}H_2O$ 2.5, $MgCl_2{\cdot}7H_2O$ 1.2, $NaHCO_3$ 24, KH_2PO_4 1.2, glucose 11, EDTA 0.5. Perfusion medium was passed through water-jacketed tubing and cylinders, and the temperature was maintained at 37°C with a temperature-controlled circulating water bath. Normal perfusion was maintained for 15 minutes and hearts were then either perfused for a further 30 minutes for control conditions or exposed to no-flow ischemia for 30 minutes. Immediately after Langendorff procedure, hearts were placed in cryovials and snap-frozen in liquid nitrogen for biochemical studies. For cryosectioning, hearts were embedded in OCT (Sakura Finotek) and snap-frozen by immersing in liquid nitrogen-chilled isopentane to snap-freeze before storage at −80°C.

Immunofluorescence

Cells were fixed with 4 % paraformaldehyde in PBS for 30 minutes and immunostained for Cx43 (rabbit polyclonal, 1/3000, Sigma-Aldrich) with cell membranes identified using wheat germ agglutinin (WGA) AlexaFluor647 (Life Technologies) as previously described (18). Cell-cell junctions in NMVMs were identified with N-cadherin (mouse monoclonal, 1/200, BD Biosciences). Slides were mounted with ProLong Gold containing DAPI (Life Technologies) for image acquisition.

Tissue cryosections (8 μm) were prepared on poly-L-lysine coated glass slides and fixed with ice-cold acetone for 5 minutes prior to air drying. Immunofluorescence was performed using antibodies directed against: Cx43 (rabbit, 1:3000), pCx43^{Ser368} (rabbit, 1/500, Cell Signaling), 14-3-3 (mouse, 1/500, Abcam), and N-cadherin (mouse, 1/200, BD Biosciences). Coverslips were mounted with ProLong Gold containing DAPI and allowed to dry overnight prior to image acquisition.

Confocal imaging was performed using a Nikon T*i* microscope, Yokogowa CSU-X1 spinning disk confocal unit with 486-, 561-, and 647-nm DPSS laser source, and Coolsnap HQ^2 camera controlled by NIS Elements software.

ImageJ software was used for quantification of Cx43 expression at intercalated discs. Briefly, background was subtracted from N-cadherin images, to which equal thresholds were applied. Resulting binary masks of intercalated disc regions were image-multiplied by corresponding Cx43 images, and fluorescence intensity was subsequently measured (11, 18). Quantification of Cx43 at cell-cell borders following knockdown of 14-3-3τ was performed as previously described utilizing fluorescence intensity profiles of 10 μm lines bisecting cell-cell borders (18, 60).

Fractionation of junctional and non-junctional Cx43

Total, junctional, and non-junctional Cx43 were fractionated from Langendorff-perfused mouse heart tissue based upon Triton-X-100 solubility. Ventricular tissue was homogenized (50 mg/ml) in 1% Triton-X-100 solubility buffer (1% Triton-X-100, 50 mM Tris 7.4, 2 mM EDTA, 2 mM EGTA, 250 mM NaCl, 1 mM NaF, 0.1 mM Na_3VO_4) supplemented with HALT inhibitor cocktail (Pierce). For ‘total fraction’, 100 μl was mixed 50/50 with 2X NuPAGE sample buffer supplemented with 200 mM DTT, sonicated, and clarified by centrifugation. Remaining lysate was centrifuged at 15,000 x *g* for 30 minutes, and the ‘soluble fraction’ supernatant removed. Pellets were weighed and resuspended at 100 μg/μl in 1X NuPAGE sample buffer supplemented with 100 mM DTT. For detection of phosphorylation at Ser373 soluble fractions were mixed 50/50 with 2X RIPA buffer and immunoprecipitation was performed as described below.

Immunoprecipitation

RIPA lysates from cells or mouse tissue were sonicated and clarified by centrifugation prior to protein concentration determination and normalization. Cx43 was immunoprecipitated from 500 μg protein using 2 μg rabbit anti Cx43 (Sigma-Aldrich) and Dynabeads protein G as previously described (18). Western blots were probed with mouse-anti 14-3-3 mode 1 (1/500, Cell Signaling), or mouse anti-ubiquitin (1/200, SantaCruz Biotechnology) stripped using Re-Blot Plus Strong Solution (Millipore), and re-probed for total Cx43 with rabbit anti-Cx43 (1/3000, Sigma).

Statistics

Prism 5 software (Graphpad) was used for all statistical analysis. The Student’s unpaired *t* test was employed to compare groups. Values represent mean ± SEM. *$P < 0.05$, **$P < 0.01$, ***$P < 0.001$.

Acknowledgments

The authors are grateful to Tina Fong (UCSF) for technical assistance. This work was supported in part by an American Heart Association Scientist Development grant 10SDG3429942 (J.W.S.) and National Institutes of Health grant HL094414 (R.M.S.).

References

1. Rohr S. Role of gap junctions in the propagation of the cardiac action potential. Cardiovascular research. 2004; 62(2):309–322. [PubMed: 15094351]
2. Shaw RM, Rudy Y. Ionic mechanisms of propagation in cardiac tissue. Roles of the sodium and L-type calcium currents during reduced excitability and decreased gap junction coupling. Circ Res. 1997; 81(5):727–741. [PubMed: 9351447]
3. Unwin PN, Zampighi G. Structure of the junction between communicating cells. Nature. 1980; 283(5747):545–549. [PubMed: 7354837]
4. Beyer EC, Paul DL, Goodenough DA. Connexin43: a protein from rat heart homologous to a gap junction protein from liver. J Cell Biol. 1987; 105(6 Pt 1):2621–2629. [PubMed: 2826492]
5. Akar FG, Nass RD, Hahn S, Cingolani E, Shah M, Hesketh GG, DiSilvestre D, Tunin RS, Kass DA, Tomaselli GF. Dynamic changes in conduction velocity and gap junction properties during development of pacing-induced heart failure. Am J Physiol Heart Circ Physiol. 2007; 293(2):H1223–1230. [PubMed: 17434978]
6. Beardslee MA, Lerner DL, Tadros PN, Laing JG, Beyer EC, Yamada KA, Kleber AG, Schuessler RB, Saffitz JE. Dephosphorylation and intracellular redistribution of ventricular connexin43 during electrical uncoupling induced by ischemia. Circ Res. 2000; 87(8):656–662. [PubMed: 11029400]
7. Luke RA, Saffitz JE. Remodeling of ventricular conduction pathways in healed canine infarct border zones. J Clin Invest. 1991; 87(5):1594–1602. [PubMed: 2022731]
8. Smith JH, Green CR, Peters NS, Rothery S, Severs NJ. Altered patterns of gap junction distribution in ischemic heart disease. An immunohistochemical study of human myocardium using laser scanning confocal microscopy. Am J Pathol. 1991; 139(4):801–821. [PubMed: 1656760]
9. Kalcheva N, Qu J, Sandeep N, Garcia L, Zhang J, Wang Z, Lampe PD, Suadicani SO, Spray DC, Fishman GI. Gap junction remodeling and cardiac arrhythmogenesis in a murine model of oculodentodigital dysplasia. Proc Natl Acad Sci U S A. 2007; 104(51):20512–20516. [PubMed: 18077386]
10. Peters NS, Coromilas J, Severs NJ, Wit AL. Disturbed connexin43 gap junction distribution correlates with the location of reentrant circuits in the epicardial border zone of healing canine infarcts that cause ventricular tachycardia. Circulation. 1997; 95(4):988–996. [PubMed: 9054762]
11. Smyth JW, Hong TT, Gao D, Vogan JM, Jensen BC, Fong TS, Simpson PC, Stainier DY, Chi NC, Shaw RM. Limited forward trafficking of connexin 43 reduces cell-cell coupling in stressed human and mouse myocardium. J Clin Invest. 2010; 120(1):266–279. [PubMed: 20038810]
12. Hesketh GG, Van Eyk JE, Tomaselli GF. Mechanisms of gap junction traffic in health and disease. J Cardiovasc Pharmacol. 2009; 54(4):263–272. [PubMed: 19701097]
13. Smyth, JW.; Shaw, RM. Heart Rhythm. 2011. The gap junction life cycle.
14. Thevenin AF, Kowal TJ, Fong JT, Kells RM, Fisher CG, Falk MM. Proteins and mechanisms regulating gap-junction assembly, internalization, and degradation. Physiology. 2013; 28(2):93–116. [PubMed: 23455769]
15. Beardslee MA, Laing JG, Beyer EC, Saffitz JE. Rapid turnover of connexin43 in the adult rat heart. Circ Res. 1998; 83(6):629–635. [PubMed: 9742058]
16. Jordan K, Solan JL, Dominguez M, Sia M, Hand A, Lampe PD, Laird DW. Trafficking, assembly, and function of a connexin43-green fluorescent protein chimera in live mammalian cells. Mol Biol Cell. 1999; 10(6):2033–2050. [PubMed: 10359613]
17. Shaw RM, Fay AJ, Puthenveedu MA, von Zastrow M, Jan YN, Jan LY. Microtubule plus-end-tracking proteins target gap junctions directly from the cell interior to adherens junctions. Cell. 2007; 128(3):547–560. [PubMed: 17289573]

18. Smyth JW, Vogan JM, Buch PJ, Zhang SS, Fong TS, Hong TT, Shaw RM. Actin cytoskeleton rest stops regulate anterograde traffic of connexin 43 vesicles to the plasma membrane. Circ Res. 2012; 110(7):978–989. [PubMed: 22328533]
19. D'Hondt C, Iyyathurai J, Vinken M, Rogiers V, Leybaert L, Himpens B, Bultynck G. Regulation of connexin- and pannexin-based channels by post-translational modifications. Biology of the cell / under the auspices of the European Cell Biology Organization. 2013; 105(9):373–398. [PubMed: 23718186]
20. Marquez-Rosado L, Solan JL, Dunn CA, Norris RP, Lampe PD. Connexin43 phosphorylation in brain, cardiac, endothelial and epithelial tissues. Biochim Biophys Acta. 2012; 1818(8):1985–1992. [PubMed: 21819962]
21. Paulson AF, Lampe PD, Meyer RA, TenBroek E, Atkinson MM, Walseth TF, Johnson RG. Cyclic AMP and LDL trigger a rapid enhancement in gap junction assembly through a stimulation of connexin trafficking. J Cell Sci. 2000; 113 (Pt 17):3037–3049. [PubMed: 10934042]
22. TenBroek EM, Lampe PD, Solan JL, Reynhout JK, Johnson RG. Ser364 of connexin43 and the upregulation of gap junction assembly by cAMP. The Journal of cell biology. 2001; 155(7):1307–1318. [PubMed: 11756479]
23. Cooper CD, Lampe PD. Casein kinase 1 regulates connexin-43 gap junction assembly. The Journal of biological chemistry. 2002; 277(47):44962–44968. [PubMed: 12270943]
24. Solan JL, Lampe PD. Connexin phosphorylation as a regulatory event linked to gap junction channel assembly. Biochim Biophys Acta. 2005; 1711(2):154–163. [PubMed: 15955300]
25. Remo BF, Qu J, Volpicelli FM, Giovannone S, Shin D, Lader J, Liu FY, Zhang J, Lent DS, Morley GE, Fishman GI. Phosphatase-resistant gap junctions inhibit pathological remodeling and prevent arrhythmias. Circ Res. 2011; 108(12):1459–1466. [PubMed: 21527737]
26. Cameron SJ, Malik S, Akaike M, Lerner-Marmarosh N, Yan C, Lee JD, Abe J, Yang J. Regulation of epidermal growth factor-induced connexin 43 gap junction communication by big mitogen-activated protein kinase1/ERK5 but not ERK1/2 kinase activation. J Biol Chem. 2003; 278(20): 18682–18688. [PubMed: 12637502]
27. Cottrell GT, Lin R, Warn-Cramer BJ, Lau AF, Burt JM. Mechanism of v-Src- and mitogen-activated protein kinase-induced reduction of gap junction communication. American journal of physiology Cell physiology. 2003; 284(2):C511–520. [PubMed: 12388103]
28. Sirnes S, Kjenseth A, Leithe E, Rivedal E. Interplay between PKC and the MAP kinase pathway in Connexin43 phosphorylation and inhibition of gap junction intercellular communication. Biochemical and biophysical research communications. 2009; 382(1):41–45. [PubMed: 19258009]
29. Warn-Cramer BJ, Cottrell GT, Burt JM, Lau AF. Regulation of connexin-43 gap junctional intercellular communication by mitogen-activated protein kinase. J Biol Chem. 1998; 273(15): 9188–9196. [PubMed: 9535909]
30. Warn-Cramer BJ, Lampe PD, Kurata WE, Kanemitsu MY, Loo LW, Eckhart W, Lau AF. Characterization of the mitogen-activated protein kinase phosphorylation sites on the connexin-43 gap junction protein. The Journal of biological chemistry. 1996; 271(7):3779–3786. [PubMed: 8631994]
31. Solan JL, Lampe PD. Specific Cx43 phosphorylation events regulate gap junction turnover in vivo. FEBS Lett. 2014
32. Lampe PD, TenBroek EM, Burt JM, Kurata WE, Johnson RG, Lau AF. Phosphorylation of connexin43 on serine368 by protein kinase C regulates gap junctional communication. J Cell Biol. 2000; 149(7):1503–1512. [PubMed: 10871288]
33. Leithe E, Rivedal E. Ubiquitination and down-regulation of gap junction protein connexin-43 in response to 12-O-tetradecanoylphorbol 13-acetate treatment. Journal of Biological Chemistry. 2004; 279(48):50089–50096. [PubMed: 15371442]
34. Moreno AP, Fishman GI, Spray DC. Phosphorylation shifts unitary conductance and modifies voltage dependent kinetics of human connexin43 gap junction channels. Biophysical journal. 1992; 62(1):51–53. [PubMed: 1376174]
35. Moreno AP, Saez JC, Fishman GI, Spray DC. Human connexin43 gap junction channels. Regulation of unitary conductances by phosphorylation. Circ Res. 1994; 74(6):1050–1057. [PubMed: 7514508]

36. Cone AC, Cavin G, Ambrosi C, Hakozaki H, Wu-Zhang AX, Kunkel MT, Newton AC, Sosinsky GE. Protein Kinase Cdelta-Mediated Phosphorylation of Connexin43 Gap Junction Channels Causes Movement within Gap Junctions followed by Vesicle Internalization and Protein Degradation. J Biol Chem. 2014
37. Fong JT, Nimlamool W, Falk MM. EGF induces efficient Cx43 gap junction endocytosis in mouse embryonic stem cell colonies via phosphorylation of Ser262, Ser279/282, and Ser368. FEBS Lett. 2014
38. Miura T, Yano T, Naitoh K, Nishihara M, Miki T, Tanno M, Shimamoto K. Delta-opioid receptor activation before ischemia reduces gap junction permeability in ischemic myocardium by PKC-epsilon-mediated phosphorylation of connexin 43. American journal of physiology. 2007; 293(3):H1425–1431. [PubMed: 17513490]
39. O'Quinn MP, Palatinus JA, Harris BS, Hewett KW, Gourdie RG. A peptide mimetic of the connexin43 carboxyl terminus reduces gap junction remodeling and induced arrhythmia following ventricular injury. Circ Res. 2011; 108(6):704–715. [PubMed: 21273554]
40. Palatinus JA, Rhett JM, Gourdie RG. Enhanced PKCepsilon mediated phosphorylation of connexin43 at serine 368 by a carboxyl-terminal mimetic peptide is dependent on injury. Channels. 2011; 5(3):236–240. [PubMed: 21532342]
41. Solan JL, Marquez-Rosado L, Sorgen PL, Thornton PJ, Gafken PR, Lampe PD. Phosphorylation at S365 is a gatekeeper event that changes the structure of Cx43 and prevents down-regulation by PKC. J Cell Biol. 2007; 179(6):1301–1309. [PubMed: 18086922]
42. Park DJ, Freitas TA, Wallick CJ, Guyette CV, Warn-Cramer BJ. Molecular dynamics and in vitro analysis of Connexin43: A new 14-3-3 mode-1 interacting protein. Protein Sci. 2006; 15(10): 2344–2355. [PubMed: 17008717]
43. Park DJ, Wallick CJ, Martyn KD, Lau AF, Jin C, Warn-Cramer BJ. Akt phosphorylates Connexin43 on Ser373, a "mode-1" binding site for 14-3-3. Cell Commun Adhes. 2007; 14(5): 211–226. [PubMed: 18163231]
44. Zuzarte M, Heusser K, Renigunta V, Schlichthorl G, Rinne S, Wischmeyer E, Daut J, Schwappach B, Preisig-Muller R. Intracellular traffic of the K+ channels TASK-1 and TASK-3: role of N- and C-terminal sorting signals and interaction with 14-3-3 proteins. J Physiol. 2009; 587(Pt 5):929–952. [PubMed: 19139046]
45. Smith AJ, Daut J, Schwappach B. Membrane proteins as 14-3-3 clients in functional regulation and intracellular transport. Physiology. 2011; 26(3):181–191. [PubMed: 21670164]
46. O'Kelly I, Butler MH, Zilberberg N, Goldstein SA. Forward transport. 14-3-3 binding overcomes retention in endoplasmic reticulum by dibasic signals. Cell. 2002; 111(4):577–588. [PubMed: 12437930]
47. Batra N, Riquelme MA, Burra S, Jiang JX. 14-3-3theta Facilitates plasma membrane delivery and function of mechanosensitive connexin 43 hemichannels. Journal of cell science. 2013
48. Majoul IV, Onichtchouk D, Butkevich E, Wenzel D, Chailakhyan LM, Duden R. Limiting transport steps and novel interactions of Connexin-43 along the secretory pathway. Histochemistry and cell biology. 2009; 132(3):263–280. [PubMed: 19626334]
49. Dunn CA, Lampe PD. Injury-triggered Akt phosphorylation of Cx43: a ZO-1-driven molecular switch that regulates gap junction size. Journal of cell science. 2013
50. Wang B, Yang H, Liu YC, Jelinek T, Zhang L, Ruoslahti E, Fu H. Isolation of high-affinity peptide antagonists of 14-3-3 proteins by phage display. Biochemistry. 1999; 38(38):12499–12504. [PubMed: 10493820]
51. Obsil T, Obsilova V. Structural basis of 14-3-3 protein functions. Seminars in cell & developmental biology. 2011; 22(7):663–672. [PubMed: 21920446]
52. Solan JL, Lampe PD. Key connexin 43 phosphorylation events regulate the gap junction life cycle. J Membr Biol. 2007; 217(1–3):35–41. [PubMed: 17629739]
53. Ek-Vitorin JF, King TJ, Heyman NS, Lampe PD, Burt JM. Selectivity of connexin 43 channels is regulated through protein kinase C-dependent phosphorylation. Circ Res. 2006; 98(12):1498–1505. [PubMed: 16709897]
54. Macia E, Ehrlich M, Massol R, Boucrot E, Brunner C, Kirchhausen T. Dynasore, a cell-permeable inhibitor of dynamin. Dev Cell. 2006; 10(6):839–850. [PubMed: 16740485]

55. Leithe E, Rivedal E. Epidermal growth factor regulates ubiquitination, internalization and proteasome-dependent degradation of connexin43. Journal of Cell Science. 2004; 117(Pt 7):1211–1220. [PubMed: 14970263]
56. Steinberg MS, McNutt PM. Cadherins and their connections: adhesion junctions have broader functions. Curr Opin Cell Biol. 1999; 11(5):554–560. [PubMed: 10508659]
57. Maass K, Shibayama J, Chase SE, Willecke K, Delmar M. C-terminal truncation of connexin43 changes number, size, and localization of cardiac gap junction plaques. Circ Res. 2007; 101(12): 1283–1291. [PubMed: 17932323]
58. Maass K, Chase SE, Lin X, Delmar M. Cx43 CT domain influences infarct size and susceptibility to ventricular tachyarrhythmias in acute myocardial infarction. Cardiovasc Res. 2009; 84(3):361–367. [PubMed: 19620131]
59. Lubkemeier I, Requardt RP, Lin X, Sasse P, Andrie R, Schrickel JW, Chkourko H, Bukauskas FF, Kim JS, Frank M, Malan D, Zhang J, Wirth A, Dobrowolski R, Mohler PJ, et al. Deletion of the last five C-terminal amino acid residues of connexin43 leads to lethal ventricular arrhythmias in mice without affecting coupling via gap junction channels. Basic Res Cardiol. 2013; 108(3):348. [PubMed: 23558439]
60. Smyth JW, Shaw RM. Autoregulation of connexin43 gap junction formation by internally translated isoforms. Cell Rep. 2013; 5(3):611–618. [PubMed: 24210816]
61. Rhett JM, Veeraraghavan R, Poelzing S, Gourdie RG. The perinexus: sign-post on the path to a new model of cardiac conduction? Trends in cardiovascular medicine. 2013; 23(6):222–228. [PubMed: 23490883]
62. Rhett JM, Ongstad EL, Jourdan J, Gourdie RG. Cx43 associates with Na(v)1. 5 in the cardiomyocyte perinexus. J Membr Biol. 2012; 245(7):411–422. [PubMed: 22811280]
63. Agullo-Pascual E, Delmar M. The noncanonical functions of Cx43 in the heart. J Membr Biol. 2012; 245(8):477–482. [PubMed: 22825715]
64. Gumpert AM, Varco JS, Baker SM, Piehl M, Falk MM. Double-membrane gap junction internalization requires the clathrin-mediated endocytic machinery. FEBS Lett. 2008; 582(19): 2887–2892. [PubMed: 18656476]
65. Piehl M, Lehmann C, Gumpert A, Denizot JP, Segretain D, Falk MM. Internalization of large double-membrane intercellular vesicles by a clathrin-dependent endocytic process. Mol Biol Cell. 2007; 18(2):337–347. [PubMed: 17108328]
66. Boassa D, Solan JL, Papas A, Thornton P, Lampe PD, Sosinsky GE. Trafficking and recycling of the connexin43 gap junction protein during mitosis. Traffic. 2010; 11(11):1471–1486. [PubMed: 20716111]
67. Giepmans BN. Gap junctions and connexin-interacting proteins. Cardiovascular research. 2004; 62(2):233–245. [PubMed: 15094344]
68. Giepmans BN, Moolenaar WH. The gap junction protein connexin43 interacts with the second PDZ domain of the zona occludens-1 protein. Curr Biol. 1998; 8(16):931–934. [PubMed: 9707407]
69. Laing JG, Chou BC, Steinberg TH. ZO-1 alters the plasma membrane localization and function of Cx43 in osteoblastic cells. Journal of cell science. 2005; 118(Pt 10):2167–2176. [PubMed: 15855237]
70. Rhett JM, Jourdan J, Gourdie RG. Connexin 43 connexon to gap junction transition is regulated by zonula occludens-1. Molecular biology of the cell. 2011; 22(9):1516–1528. [PubMed: 21411628]
71. Hunter AW, Barker RJ, Zhu C, Gourdie RG. Zonula occludens-1 alters connexin43 gap junction size and organization by influencing channel accretion. Mol Biol Cell. 2005; 16(12):5686–5698. [PubMed: 16195341]
72. Hunter AW, Jourdan J, Gourdie RG. Fusion of GFP to the carboxyl terminus of connexin43 increases gap junction size in HeLa cells. Cell Commun Adhes. 2003; 10(4–6):211–214. [PubMed: 14681018]
73. Chen J, Pan L, Wei Z, Zhao Y, Zhang M. Domain-swapped dimerization of ZO-1 PDZ2 generates specific and regulatory connexin43-binding sites. The EMBO journal. 2008; 27(15):2113–2123. [PubMed: 18636092]

74. Barker RJ, Price RL, Gourdie RG. Increased association of ZO-1 with connexin43 during remodeling of cardiac gap junctions. Circ Res. 2002; 90(3):317–324. [PubMed: 11861421]

75. Bruce AF, Rothery S, Dupont E, Severs NJ. Gap junction remodelling in human heart failure is associated with increased interaction of connexin43 with ZO-1. Cardiovasc Res. 2008; 77(4):757–765. [PubMed: 18056766]

76. Kieken F, Mutsaers N, Dolmatova E, Virgil K, Wit AL, Kellezi A, Hirst-Jensen BJ, Duffy HS, Sorgen PL. Structural and Molecular Mechanisms of Gap Junction Remodeling in Epicardial Border Zone Myocytes following Myocardial Infarction. Circ Res. 2009

Synopsis

Cardiac ischemia rapidly leads to alterations in phosphorylation status and altered localization of connexin 43 (Cx43) gap junctions, resulting in ventricular arrhythmias. In this study, we find that phosphorylation-mediated activation of a 14-3-3 binding motif at Ser373 within the Cx43 C-terminus is a gate-keeper event necessary for further phosphorylation and ubiquitination of Cx43, leading to endocytosis of gap junctions. Regulation of $Cx43^{Ser373}$ phosphorylation and Cx43 /14-3-3 complexing could be a therapeutic strategy to restore gap junction coupling in ischemic disease.

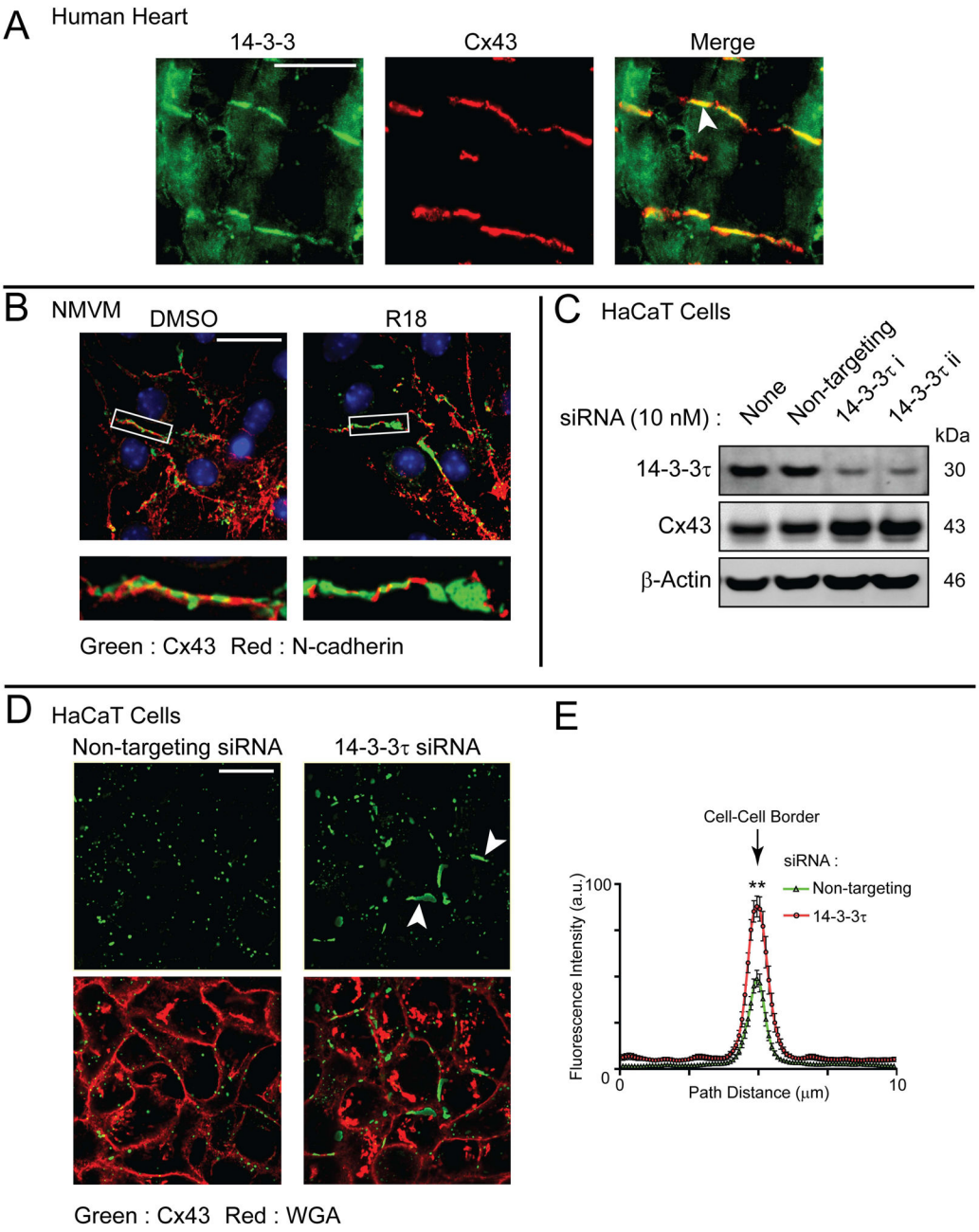

Figure 1. 14-3-3 proteins are enriched at intercalated discs of human heart and regulate Cx43 gap junction plaque size

A) Confocal immunofluorescence of a non-failing human heart cryosection probed for 14-3-3 (green) and Cx43 (red). Merged image on right includes nuclear counterstain DAPI. Original magnification: X20. Scale bar = 50 μm. B) Confocal immunofluorescence of NMCMs incubated overnight with the 14-3-3 inhibitor R18 (25 μM) or DMSO probed for Cx43 (green) and N-cadherin (red). Original magnification: X60, Scale bar = 25 μm. C) Western blot of HaCaT cells stably expressing Cx43 transfected with non-targeting siRNA (second lane) or siRNA duplexes targeting 14-3-3τ (third and fourth lanes) probed for 14-3-3τ (top panel), Cx43 (middle panel), and β-actin (bottom panel). D) Confocal

immunofluorescence of HaCaT cells stably expressing Cx43 transfected with non-targeting siRNA (left panels) or an siRNA duplex targeting 14-3-3τ (right panels) probed for Cx43 (green) and counterstained with WGA to identify cell-cell borders. Original magnification: X60. Scale bar = 25 μm. E) Fluorescence intensity profiles of Cx43 expression at cell-cell borders in D, data are averaged from 15 cell pairs. All data are representative of three separate experiments.

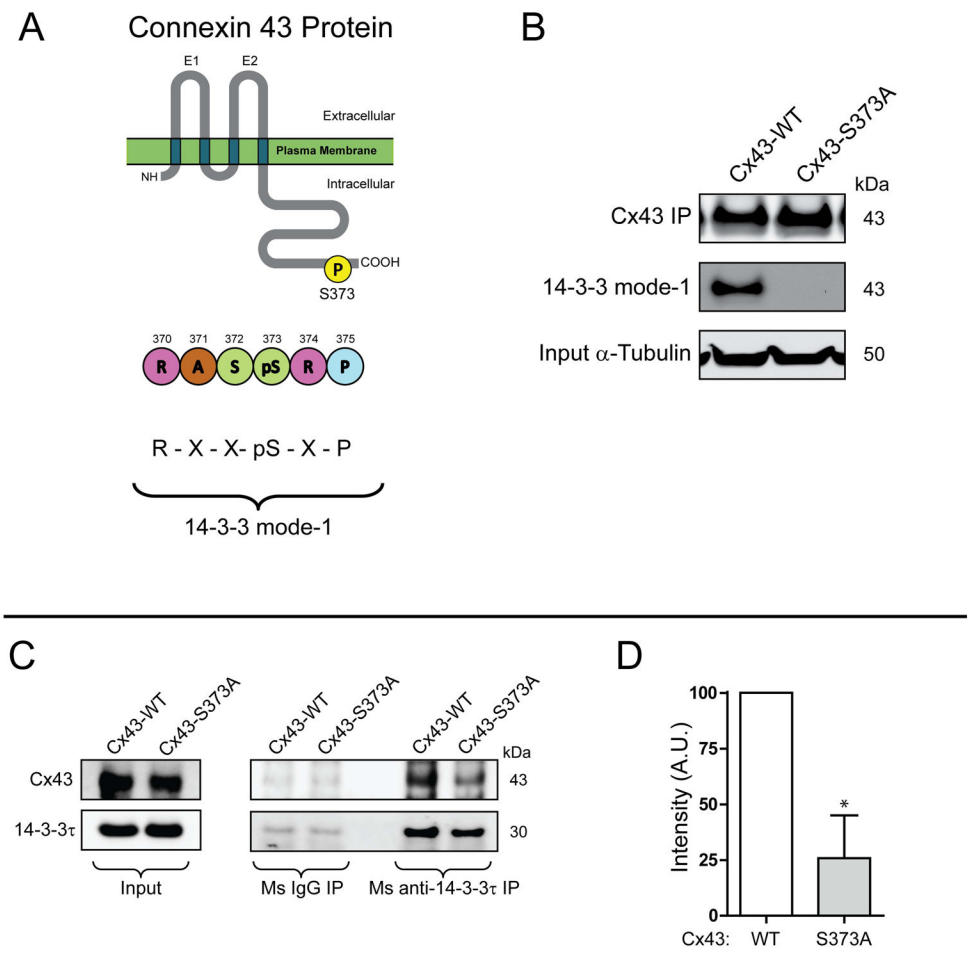

Figure 2. Cx43 contains a mode-1 14-3-3 binding motif

A) Schematic of Cx43 protein and location of 14-3-3 mode-1 binding motif. B) Western blot of Cx43 immunoprecipitation in HaCaT cells transiently transfected with wild-type Cx43 (left lane) or $Cx43^{S373A}$ probed for Cx43 (top panel), phosphorylated 14-3-3 mode-1 motif (middle panel). Input α-tubulin presented in bottom panel. C) DSP cross-linked co-immunoprecipitation of Cx43 through 14-3-3τ in HaCaT cells transiently transfected with wild-type Cx43 or $Cx43^{S373A}$. Western Blot probed for Cx43 (top panels) and 14-3-3τ (bottom panels). D) Quantification by densitometry of co-immunoprecipitation of $Cx43^{S373A}$ with 14-3-3τ in comparison to wild-type Cx43 (n = 3).

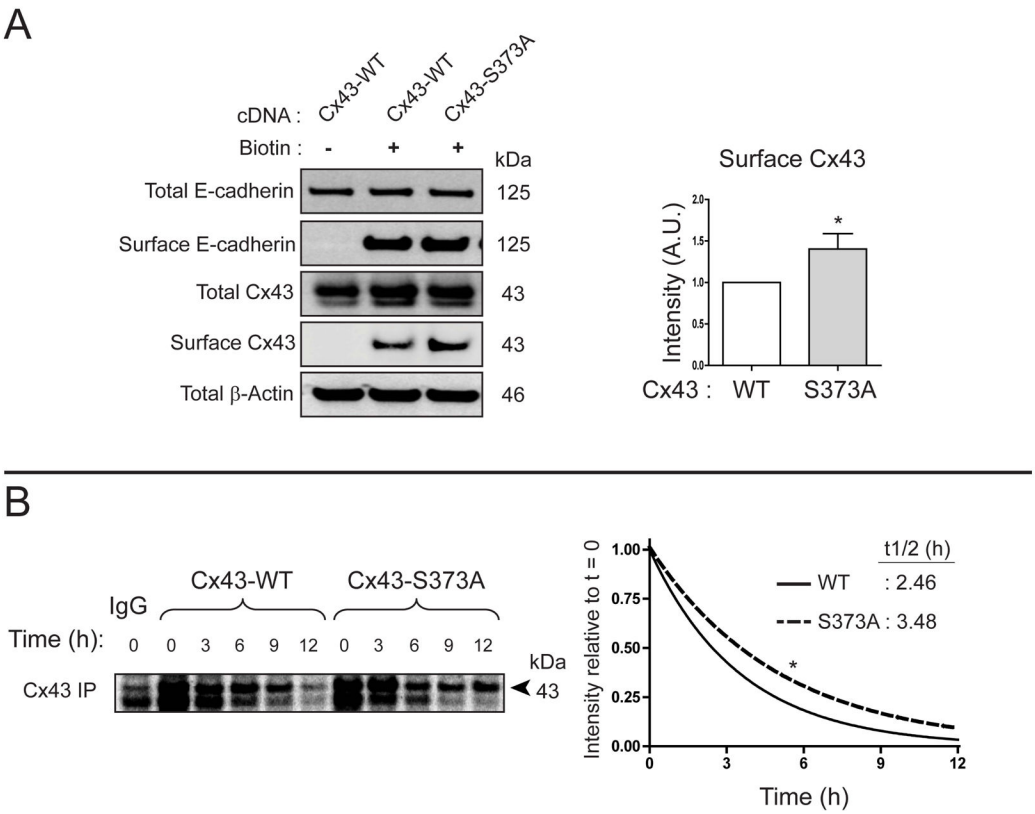

Figure 3. Inactivation of the Cx43 14-3-3 binding motif stabilizes the Cx43 protein

A) Western blot of surface protein biotinylation in HaCaT cells transiently transfected with wild-type Cx43 or Cx43^{S373A}. Densitometry of surface Cx43 levels presented in graph on right (n = 3). B) Immunoprecipitation of Cx43 from ^{35}S pulse-chase of HaCaT cells transiently transfected with wild-type Cx43 or Cx43^{S373A}. Graph on right is quantification of averaged (n = 3) intensity values relative to t = 0 for wild-type Cx43 (solid line) and Cx43-S373A (dashed line).

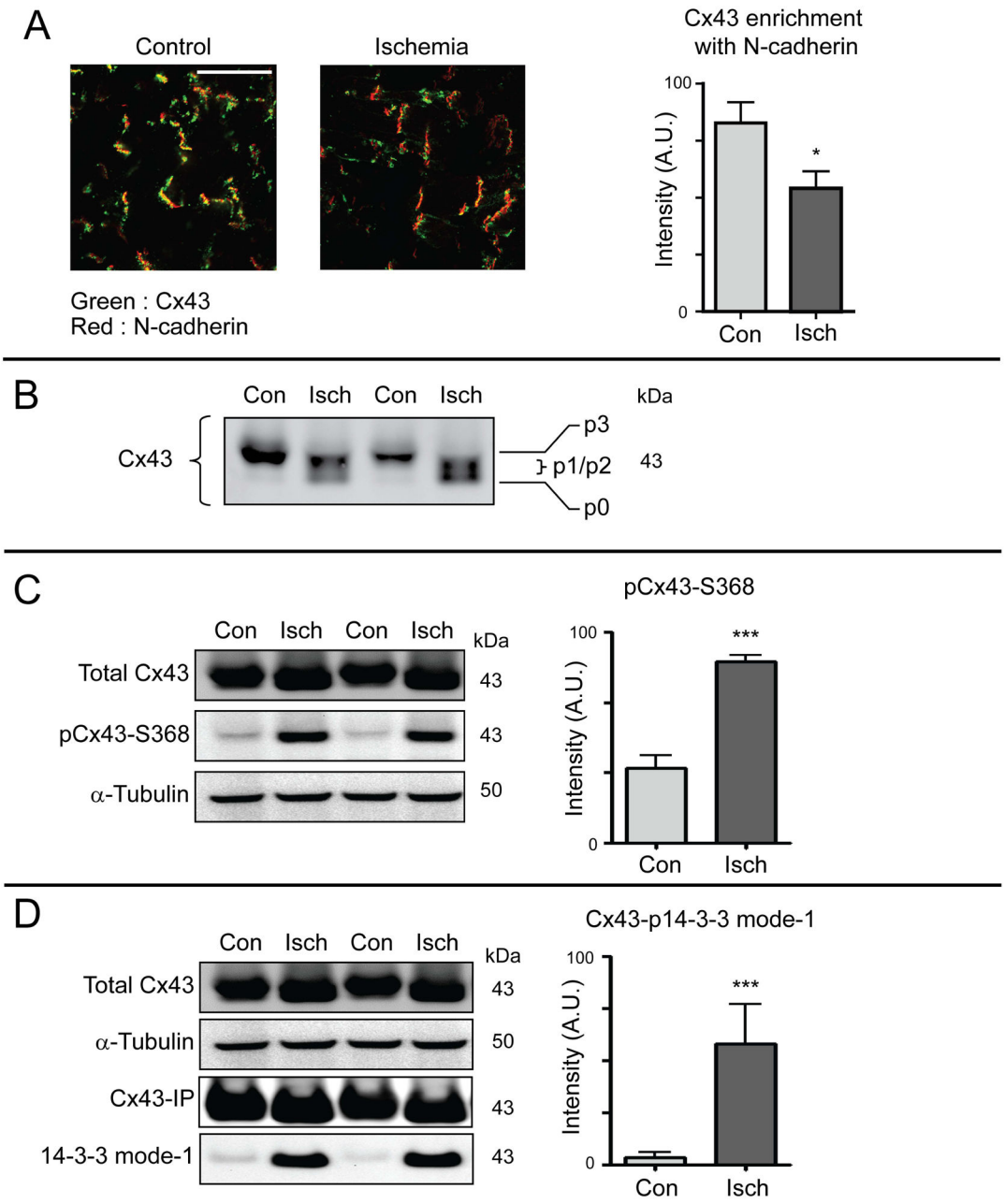

Figure 4. Acute cardiac ischemia induces hyper-phosphorylation of Cx43 at serines 368 and 373

Hearts from 8-week-old C57BL/6 mice were maintained using a Langendorff perfusion apparatus for 15 minutes, followed either by 30 minutes of normal perfusion (control) or no-flow ischemia (n = 3 per condition). A) Confocal immunofluorescence of Cx43 (green) and N-cadherin (red) in cryosections from snap-frozen hearts. Quantification of Cx43/N-cadherin colocalization in graph on right. Original magnification: X60. Scale bar = 50 μm. B) Western blot of lysates from control (con) and ischemic (isch) hearts probed for Cx43 to visualize phosphospecific forms p0 – p3. C) Western blot of lysates from control and ischemic hearts probed for total Cx43 (top panel), $pCx43^{Ser368}$ (middle panel) and α-tubulin (bottom panel). Quantification of $pCx43^{Ser368}$ relative to total Cx43 in graph on right. D)

Cx43 immunoprecipitations from control and ischemic hearts. Immunoprecipitation Western blot was probed for Cx43 and phosphorylated 14-3-3 mode-1 motif. Quantification of phosphorylated 14-3-3 mode-1 motif in graph on right.

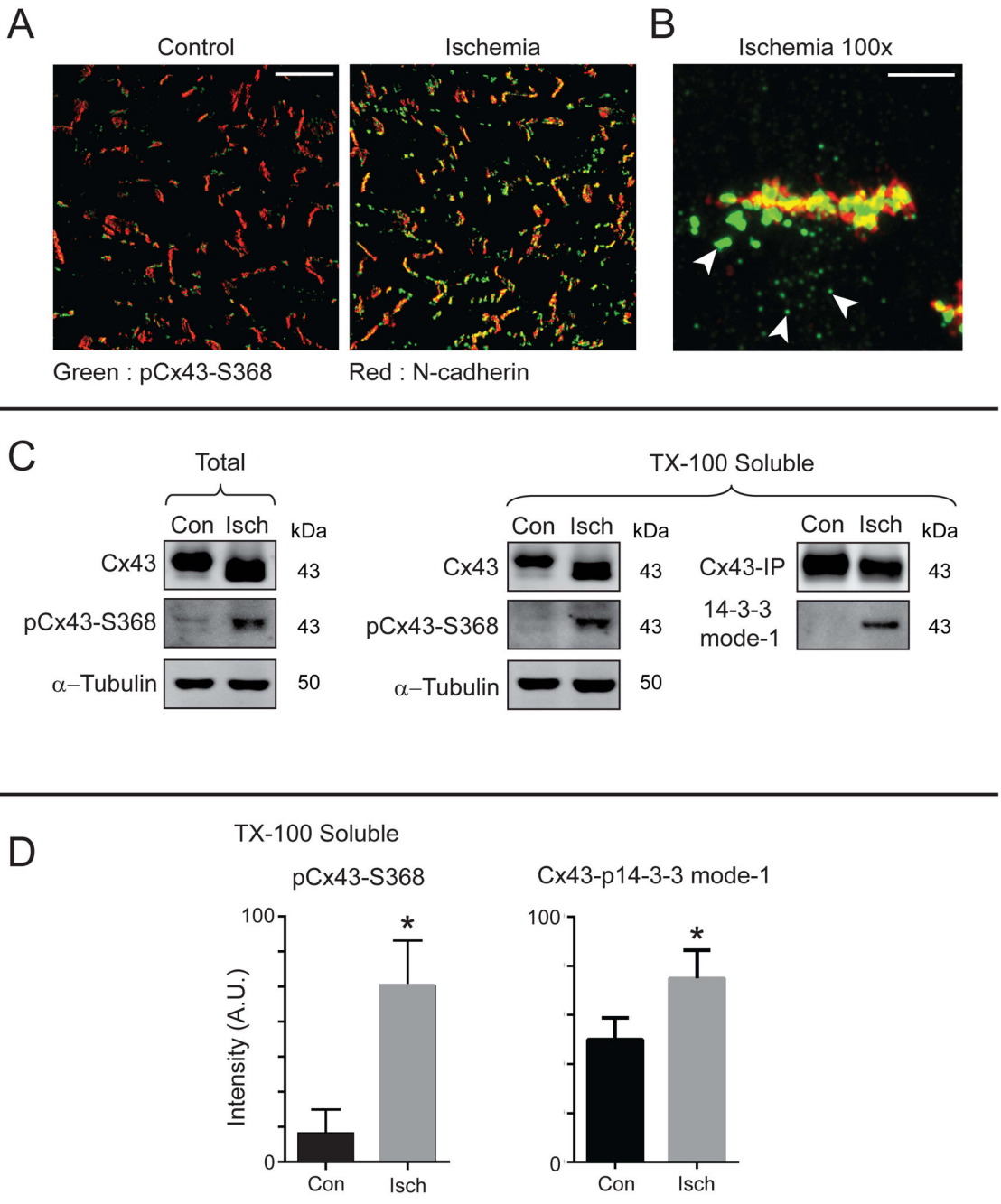

Figure 5. Serine 368/373 phosphorylated Cx43 is present in non-junctional compartments following acute ischemia

Hearts from 8-week-old C57BL/6 mice were maintained using a Langendorff perfusion apparatus for 15 minutes, followed either by 30 minutes of normal perfusion or ischemia (*n* = 3 per condition). A) Confocal immunofluorescence of pCx43^{Ser368} (green) and N-cadherin (red) in heart cryosections. Original magnification: X20. Scale bar = 50 μm. B) Zoomed in confocal immunofluorescence of an intercalated disc from an ischemic heart probed for pCx43^{Ser368} (green) and N-cadherin (red). Arrows indicate intracellular pools of pCx43^{Ser368}. Original magnification: X100. Scale bar = 5 μm. C) Western blot of

fractionated control and ischemic hearts based on Triton-X-100 solubility and probed for Cx43, pCx43^{Ser368}, α-tubulin, and N-cadherin. Cx43 immunoprecipitations from soluble fractions were probed for Cx43 and phosphorylated 14-3-3 mode-1 motif. D) Quantification of phosphorylated Cx43 relative to total Cx43 from C.

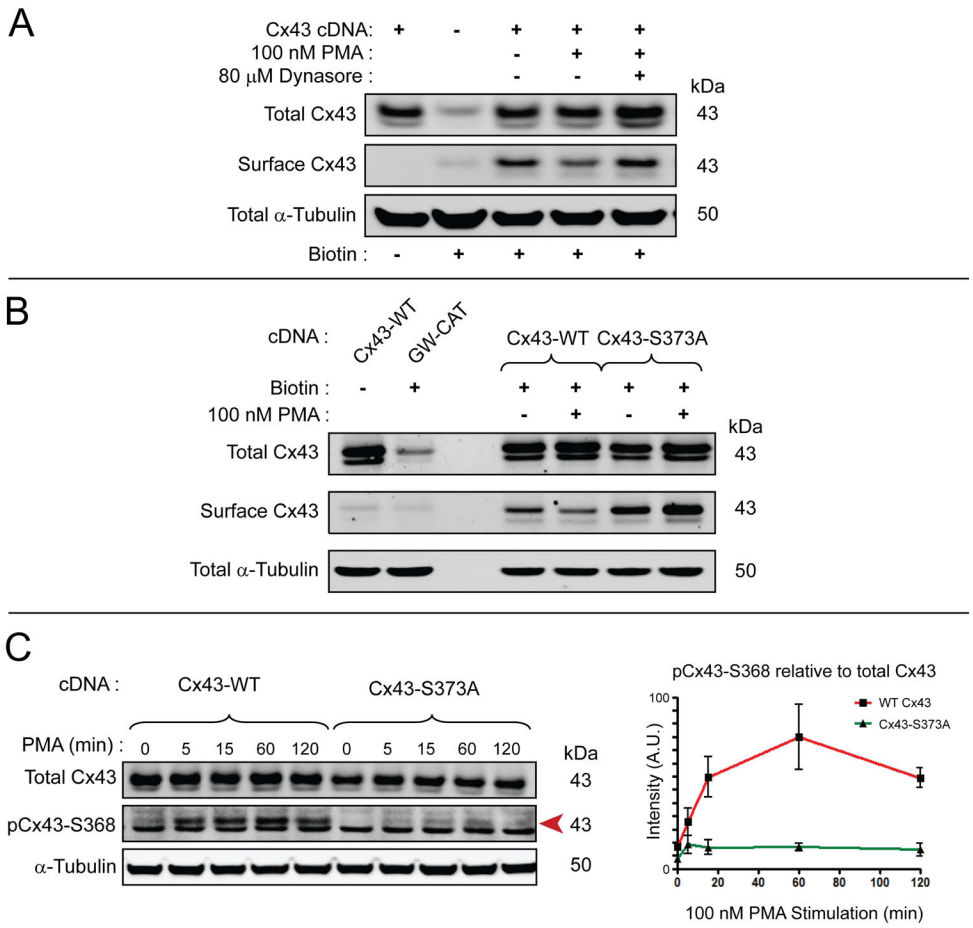

Figure 6. Cx43^{S373A} is resistant to PMA-induced internalization and phosphorylation at Ser368

A) Western blot of surface protein biotinylation in HaCaT cells transiently transfected with Cx43 incubated for 90 minutes in the presence or absence of 100 nM PMA and 80 μM Dynasore. B) Western blot of surface protein biotinylation in HaCaT cells transiently transfected with wild-type Cx43 or Cx43^{S373A} incubated for 90 minutes in the presence or absence of 100 nM PMA. C) Serum-starved HaCaT cells transiently transfected with siRNA-resistant wild-type Cx43 or Cx43^{S373A} stimulated with 100 nM PMA and harvested over 2 hours. Graph on right is quantification of pCx43^{Ser368} (red arrow on Western blot) relative to total Cx43 (n = 3). Data are representative of three separate experiments.

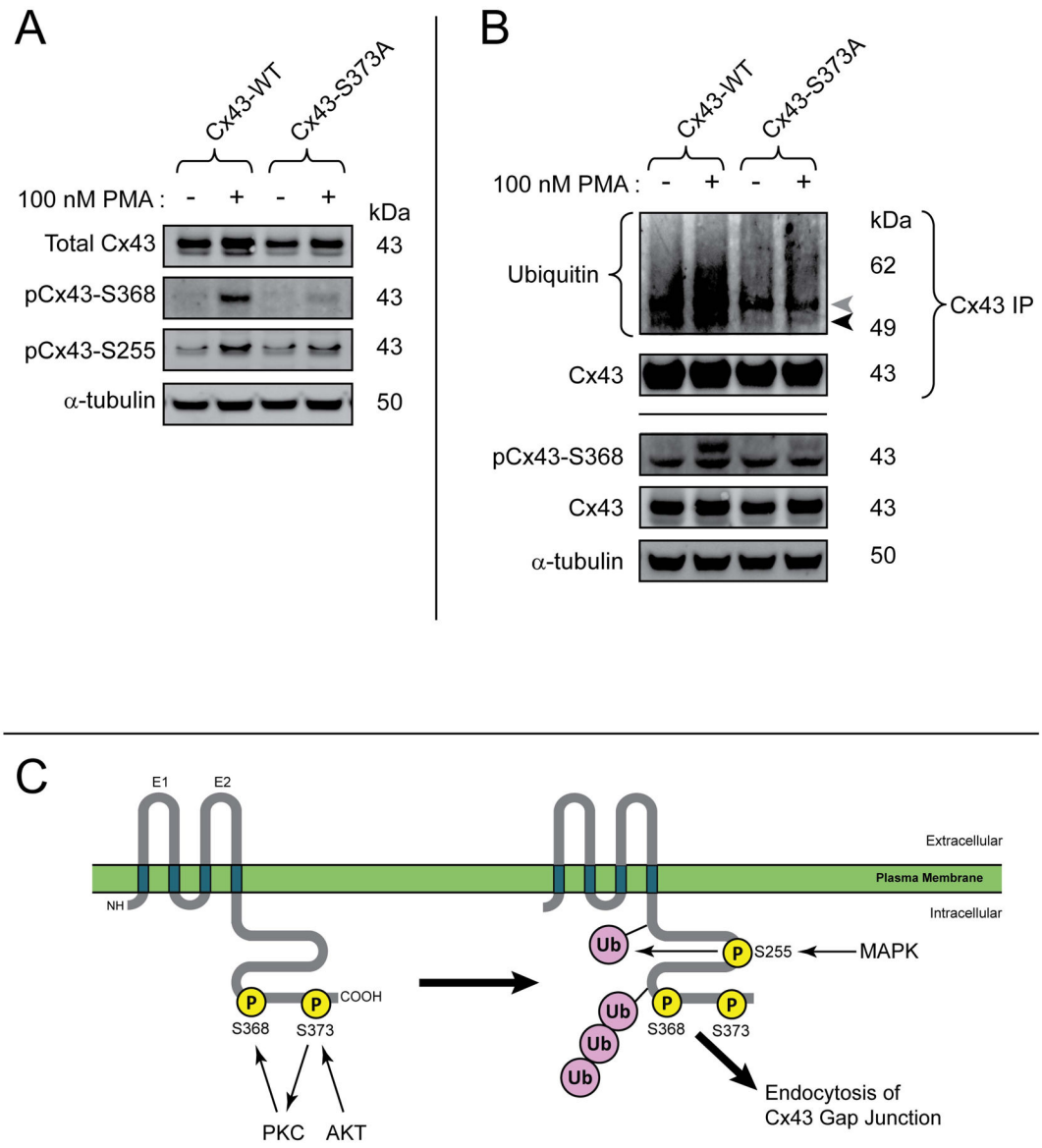

Figure 7. Cx43^{S373A} is resistant to phosphorylation at Ser368, Ser255, and ubiquitination

A) Western blot of serum-starved HaCaT cells transiently transfected with wild-type Cx43 or Cx43^{S373A} stimulated with 100 nM PMA for 15 minutes. B) Immunoprecipitation of Cx43 probed for ubiquitin to detect ubiquitinated Cx43 (black arrow). Grey arrow is IgG heavy chain. C) Schematic of sequential Cx43 phosphorylation and ubiquitination events leading to internalization. Data are representative of three separate experiments.